# Calculation of $FeO$-$TiO_2$-$Ti_2O_3$ liquidus isotherms pertaining to high titania slags

by D.J. Fourie*, J.J. Eksteen*, J.H. Zietsman†¶


## Synopsis

**During the production of pure $TiO_2$ for the pigment industry, ilmenite, containing 35–60% $TiO_2$, is reduced to high titania slag, containing 70–95% '$TiO_2$' and pig iron. The high titania slag produced, consists mainly of titanium in different oxidation states and FeO in equilibrium with liquid iron. To predict the phase and chemical reaction equilibria in a furnace, a suitable solution model is required with accurately determined binary interaction parameters, as slag melts tend to behave very non-ideally. This paper investigates two popular slag models, namely, modified quasi-Chemical (MQC) model and the cell model and provides the binary interaction parameters based on recently published data of the ternary system and critically assessed published unary and binary data. Very few modelling results have been published on the ternary Ti-Fe-O system pertaining to high titanium slags. The solution models, with their regressed interaction parameters, can subsequently be implemented in commercial software of the slag-metal phase equilibria to predict how much and which type of solids will precipitate for a given bulk slag chemistry and operating temperature or, alternatively, above which temperature should a furnace be operated to avoid excessive solids precipitation.**


## Introduction

In the high titania system the accurate estimation of the slag liquidus temperature is very important for the control of the furnace. Below the liquidus temperature, the slag viscosity increases significantly with small decreases in operating temperature, which leads to difficulties with tapping, mechanical metal entrainment and a high propensity for the slag to foam. Due to the corrosive nature of high titania slag, the furnace is operated with a freeze lining to protect the refractory against attack from the liquid slag. Keeping most of the bath above, or close to, the slag liquidus to stabilize a freeze lining, requires good control and an accurate estimation of the slag liquidus. Despite the liquidus temperature, the distribution of contaminant species between the slag and alloy phases can also be calculated by means of solution models. It is clear that solution models can be an important tool to predict the chemical properties of metallurgical systems, and with the increasing calculation power of modern computers it can be very valuable in online control. The accuracy and robustness of liquidus or phase equilibrium predictions are critically dependent on accurate pure component data and correlations, as well as accurate, thermodynamically consistent solution models, which define the thermodynamic interrelationships between components through interaction parameters.

### *Solution models can be divided into three categories[1]*

#### *Physical parameter models*

The essence of this kind of model is an inference on microstructure of slag from the measured physical properties. For example, the bonding energy of the Si–O bond is estimated according to the activation energy of viscous flow and based on the presumed relationship between microstructure and the physical properties.

#### *Thermodynamic parameter models*

The ultimate aim of these models is to deduce an equation group from the available thermodynamic data and, by means of this equation group, to evaluate interpolating and/or extrapolating. The foundation of these models is a set of presumed microstructural units. And the relationship between these units and experimental data is stipulated to follow basic principle of thermodynamics.


* *Department of Process Engineering, University of Stellenbosch, South Africa.*

† *Ex-Mente, Centurion, South Africa.*


 *SA ISSN 0038–223X/3.00 + 0.00. Paper received Jan. 2005; revised paper received Jun. 2005.*

### *Structural models*

According to this approach, the properties are related to the microstructure, which is either measured by some advanced instruments or determined along the theoretical approach of chemical bonding.

Of the three categories, the progression of this last category is the fastest. The latest developed 'cell' and 'modified quasi-chemical' models of Gaye *et al.*[2] and Pelton *et al.*[3] respectively also belong to this category and will be discussed in this paper.

## *Brief review of the relationship between the solution model and phase equilibria*

The relationship among Gibbs energies, solution models and phase diagrams is briefly reviewed here for a simple ideal binary system, as a preamble to the more complex solutions models discussed later. Consider two components A and B that are completely miscible over the entire composition range in both the liquid and solid phases (Figure 1).

At chemical equilibrium, the partial molar Gibbs free energy (chemical potential) of any component in one phase must be equal to the chemical potential of the same component in all the other phases, so that, for component *A*:

$$\overline{G}_A\left(l, x_A^1\right) = \overline{G}_A\left(s, x_A^s\right) \quad [1]$$

and for component *B*:

$$\overline{G}_B\left(l, x_B^1\right) = \overline{G}_B\left(s, x_B^s\right) \quad [2]$$

At a given temperature *T*, for component *A*:

$$\overline{G}_A(l) = \overline{G}_A^{\circ}(l) + RT \ln\ a_A(l) \quad [3]$$

$\overline{G}_A^{\circ}(l)$ is the pure component molar Gibbs free energy and $a_A(l)$ is the activity of component *A* in the given liquid phase. Correspondingly, for the solid phase:

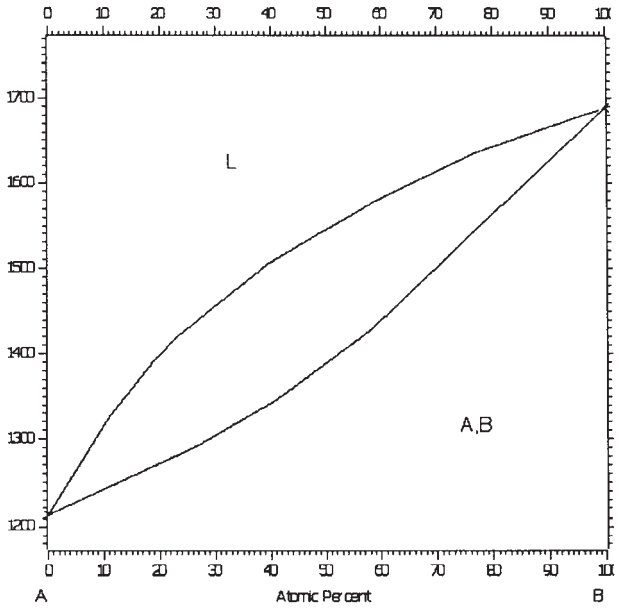


**Figure 1—Typical binary phase diagram for components A and B that are completely miscible over the entire composition range**

$$\overline{G}_A(s) = \overline{G}_A^{\circ}(s) + RT \ln\ a_A(s) \quad [4]$$

Therefore:

$$RT \ln\left[a_A(s)/a_A(l)\right] = G^{\circ}_{A(l)} - G^{\circ}_{A(s)} = \Delta G^{\circ}_{s\rightarrow l(A)} \quad [5]$$

The Gibbs free energy may be expanded in the usual manner and expressed in terms of the pure component enthalpy of melting $\Delta H^{\circ}_{mA}$, the pure component melting point $T_{mA}$, and the liquidus temperature *T*.

$$\Delta G^{\circ}_{s\rightarrow l(A)} = \Delta H^{\circ}_{mA} - T\Delta S^{\circ}_{mA} = \Delta H^{\circ}_{mA}\left(1 - T/T_{mA}\right) \quad [6]$$

Consequently:

$$\ln\left[a_A(s)/a_A(l)\right] = \left(\Delta H^{\circ}_{mA}/R\right)\left(1/T - 1/T_{mA}\right) \quad [7]$$

where:

$$a_A(l) = \gamma^l_A \cdot x^l_A \quad [8]$$

$$a_A(s) = \gamma^s_A \cdot x^s_A \quad [9]$$

where $\gamma^l_A$ is the activity coefficient of component *A*, with *x* being the mole fraction of the solute.

$$\text{Finally, } \gamma = f\left(x_{solutes}, T\right) \quad [10]$$

The activity coefficient ($\gamma$) is therefore a function of composition and temperature and can be calculated using a solution model. The liquidus curve can thus be calculated using the equations derived above. It is clear that, given the liquidus curve, the activity coefficients can be calculated as a function of composition and model parameters can be regressed. The problem of deriving solution model parameters from liquidus temperatures therefore becomes an optimization problem. The two solution models types, which have become established in thermodynamic simulation software for inorganic melts, are the cell models and the modified quasi-chemical (MQC) model, as they take into account the structural interactions in solutions. The MQC model will be discussed first as a basis for comparison, followed by the cell model, which is the focus of this paper.

## The modified quasi chemical (MQC) model

The quasi-chemical model of Guggenheim[4] for short-range ordering describes the thermodynamic properties of a system by taking structural ordering into account. Pelton *et al.*[3] later modified this model to the full MQC model.

### *Basic quasi chemical theory[3,4]*

In a binary system with components A and B, the A and B particles are considered to mix substitutionally on a quasi-lattice. The relative amounts of the three types of nearest neighbour pairs (A–A, B–B and A–B) are determined by the energy change associated with the formation of two A–B pairs from a A–A and a B–B pair:

$$\left[A-A\right]+\left[B-B\right] = 2\left[A-B\right] \quad [11]$$

If this energy change is zero, then the solution is an ideal mixture. As the energy change becomes more negative, the formation of A–B pairs is favoured. The result is then that the enthalpy of mixing tends to form a negative peak at the composition XA = XB = $^1/_2$, while the entropy of mixing has

the shape of a letter *m* as shown in Figure 2. This suggests that the maximum ordering of any binary system A–B occurs at 0.5 mole fraction.

Therefore the basic quasi-chemical theory cannot be used for silicate melts where the minimum enthalpies and entropies of mixing are not at a mole fraction of 0.5. Pelton *et al.*[3] modified the basic theory in order to provide an expression for the entropy and enthalpy of a highly ordered system with minima in entropy and enthalpy at any desired composition. As a further modification, the energy change for Reaction [11] was expressed as a function of composition with adjustable coefficients.

In the following sections, the general modified quasi-chemical theory will first be developed for binary systems and then extended to ternary systems.

### *The modified binary quasi-chemical theory*[3]

As in the basic quasi-chemical theory, a binary system with components *A* and *B* are considered where the *A* and *B* particles mix substitutionally on a quasi-lattice with a constant co-ordination number z. The three types of nearest neighbour pairs (*A–A*, *B–B* and *A–B*) have 'pair bond energies' $\varepsilon_{ij}$. The total number of such pairs per mole of solution is $N^o z/2$ where $N^o$ is Avogadro's number. The formation of two *A–B* pairs from an *A–A* and *B–B* pair according to Reaction [11] is considered. The enthalpy change for this reaction is then $(2\varepsilon_{AB}-\varepsilon_{AA}-\varepsilon_{BB})$. A molar enthalpy change $\omega$ is defined by multiplying by $N^o z/2$:

$$\omega = \frac{N^{\circ} z}{2}\left(2\varepsilon_{AB} - \varepsilon_{AA} - \varepsilon_{BB}\right) \qquad [12]$$

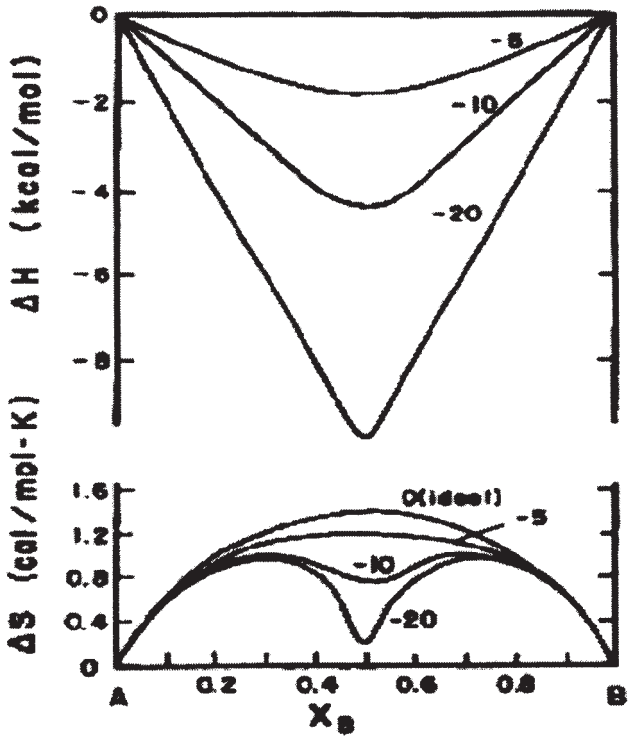


**Figure 2—Enthalpy and entropy of mixing of a binary system for different degrees of ordering about $X_A = X_B = 1/2$. Curves are calculated from the modified quasi-chemical theory at $T$ = 1000°C with $z$ = 2 for the constant values of $\omega$ (kcal) and with $\eta = 0$.[3]**

A molar non-configurational entropy change $\eta$, can also be defined:

$$\eta = \frac{N^{\circ} z}{2}\left(2\sigma_{AB} - \sigma_{AA} - \sigma_{BB}\right) \qquad [13]$$

where $\sigma_{ij}$ is the 'pair bond non-configurational entropy'.

Let $n_A$ and $n_B$ be the number of moles of *A* and *B* particles. Then, for one mole of solution, $(n_A + n_B) = 1$. The mole fractions of *A* and *B* are defined as $X_A = n_A/(n_A + n_B) = 1 - X_B$. Now let $n_{AA}$, $n_{BB}$ and $n_{AB}$ be the number of moles of each type of pair in solution. The fraction of *i–j* pairs are defined as:

$$X_{ij} = n_{ij}/\left(n_{AA} + n_{BB} + n_{AB}\right) \qquad [14]$$

from the mass balance it follows that:

$$zn_A = 2n_{AA} + n_{AB} \qquad [15]$$

$$zn_B = 2n_{BB} + n_{AB} \qquad [16]$$

and that

$$2X_A = 2X_{AA} + X_{AB} \qquad [17]$$

$$2X_B = 2X_{BB} + X_{AB} \qquad [18]$$

When components *A* and *B* are mixed, *A–B* pairs are formed at the expense of *A–A* and *B–B* pairs. The enthalpy of mixing, $\Delta H$, is given in the model by the summation of the pair bond energies:

$$\Delta H = \left(X_{AB}/2\right)\omega \qquad [19]$$

The non-configurational excess entropy of the solution is then given by:

$$\Delta S^{nonconfig} = \left(X_{AB}/2\right)\eta \qquad [20]$$

The approximate configurational entropy of mixing as proposed by Guggenheim[4], is:

$$\Delta S^{config} = -R\left(X_A \ln X_A + X_B \ln X_B\right) - \frac{Rz}{2}\left(X_{AA} \ln \frac{X_{AA}}{X_A^2} + X_{BB} \ln \frac{X_{BB}}{X_B^2} + X_{AB} \ln \frac{X_{AB}}{2X_A X_B}\right) \qquad [21]$$

Therefore, the total molar excess entropy (configurational plus non-configurational entropy) of the solution is given from Equations [20] and [21] as:

$$\Delta S^E = -\frac{Rz}{2}\left(X_{AA} \ln \frac{X_{AA}}{X_A^2} + X_{BB} \ln \frac{X_{BB}}{X_B^2} + X_{AB} \ln \frac{X_{AB}}{2X_A X_B}\right) + \left(X_{AB}/2\right)\eta \qquad [22]$$

The equilibrium concentrations are given by minimizing the Gibbs energy at constant composition:

$$\frac{\partial\left(\Delta H - T\Delta S\right)}{\partial X_{AB}} = 0 \qquad [23]$$

This gives:

$$\frac{X_{AB}^2}{X_{AA}X_{BB}} = 4e^{-2(\omega - \eta T)/zRT} \qquad [24]$$

Equation [24] resembles an equilibrium constant for Reaction [10] and therefore the model is called 'quasi-chemical'.

Substitute Equations [17] and [18] into Equation [24]:

$$X_{AB}/2 = 2X_AX_B/(1+\xi) \quad [25]$$

where

$$\xi = \left[1 + 4X_AX_B\left(e^{2(\omega-\eta T)/zRT} - 1\right)\right]^{1/2} \quad [26]$$

For a given value of ($\omega$—$\eta$T) at a given composition $X_A$, Equations [25] and [26] give $X_{AB}$ and Equations [17] and [18] then give $X_{AA}$ and $X_{BB}$. Substituting these values into Equations [19] and [22] gives $\Delta H$ and $S^E$.

In the case when, $\omega = 0$ and $\eta = 0$ it follows that $\Delta H = 0$ and $S^E = 0$ and the solution is ideal. When $\omega$ and $\eta$ are very small, $S^E \approx 0$ and $X_{AB} \approx 2X_AX_B$. Then Equation [19] becomes: $\Delta H = X_AX_B\,\omega$. In this case the solution is regular. As ($\omega$—$\eta T$) is made progressively more negative, $\Delta H$ assumes a negative peaked form as in Figure 2, and $\Delta S$ assumes the 'm-shaped' form of Figure 2. The configurational $\Delta S$ as calculated by Equation [21] assumes large negative values around $X_A = X_B = 1/2$ for large negative values of ($\omega$—$\eta T$). This is clearly incorrect since when ($\omega$—$\eta T$) = -∞, perfect ordering will result at the composition $X_A = X_B = 1/2$ with all $A$ particles having only $B$ particles as nearest neighbours and vice versa. Therefore, the configurational $\Delta S$ should be zero at this composition. The fact that the calculated configurational $\Delta$S is not zero is a result of the approximate nature of the entropy Equation [21]. If we solve the preceding equations for ($\omega$—$\eta T$) = -∞, we obtain for the configurational entropy of mixing at $X_A = X_B = 1/2$:

$$\Delta S = R\left(\frac{z}{2} - 1\right)\ln\frac{1}{2} \quad [27]$$

This will only be equal to zero when $z = 2$.

For highly ordered systems, the model therefore gives the correct entropy expression only when $z = 2$. This can be more fully understood if it is realized that Equation [21] with $z = 2$ is, in fact, the solution of the one-dimensional Ising model. Consider a one-dimensional 'necklace' of $n_A$ particles of type $A$ and $n_B$ particles of type $B$ with $n_{AA}$, $n_{BB}$ and $n_{AB}$ being the numbers of $A$–$A$, $B$–$B$ and $A$–$B$ pairs. Now place the $n_A$ particles of type $A$ in a ring and choose at random ($n_A$-$n_{AA}$) of the $n_A$ spaces between them. This choice can be made in $\Omega_A = n_A!/(n_{AA}!(n_A - n_{AA})!)$ ways. We now place one particle of type $B$ in each of these chosen spaces. This leaves $n_B - (n_A - n_{AA}) = n_{BB}$ particles of type $B$. These are all placed into the ($n_A$–$n_{AA}$) chosen spaces with no restriction on the number in each space. This can be done in $\Omega_B = n_B!/(n_{BB}!(n_B - n_{BB})!)$ ways since ($n_A$–$n_{AA}$) = ($n_B$–$n_{BB}$). The entropy is then given by:

$$\Delta S = -k\ln\Omega_A\Omega_B \quad [28]$$

where $k$ is Boltzmann's constant.

Solving for one mole of particles gives an expression for $\Delta$S identical to that of Equation [21] with $z = 2$. Hence, the model as presented is exact in one-dimension ($z = 2$). Thus, for highly ordered systems, the correct entropy is only approached by the model when $z = 2$. For solutions that are only slightly ordered ($S^E \approx 0$), it may be argued that the approximate three-dimensional expression is superior to the exact one-dimensional expression and so a larger value of $z$ should be used.

### *Fixing the composition of maximum ordering*

The next modification to the model concerns the composition of maximum ordering. As presented above, the model always gives maximum ordering at $X_A = X_B = 1/2$. In order to make the model general, we must be able to choose the composition of maximum ordering to correspond to that which is observed. For instance, in the binary system $MgO$–$SiO_2$, this composition is observed near $X_{MgO} = 2/3$, $X_{SiO2} = 1/3$ (corresponding to $Mg_2SiO_4$). The simplest means of accomplishing this is to replace the mole fractions $X_A$ and $X_B$ in the preceding equations by equivalent fractions, $Y_A$ and $Y_B$ defined by:

$$Y_A = \frac{aX_A}{aX_A + bX_B} \quad [29]$$

$$Y_B = \frac{bX_B}{aX_A + bX_B} \quad [30]$$

Where $a$ and $b$ are numbers chosen so that $Y_A = Y_B = 1/2$ at the composition of maximum ordering. For example, in the $MgO$–$SiO_2$ system, by choosing $a$ and $b$ such that $a/(a + b) = 1/3$ (for example, by choosing $a = 1$, $b = 2$), we obtain $Y_A = Y_B = 1/2$ when $X_A = 2/3$ and $X_B = 1/3$. Formally, in the model, we let the coordination numbers of $A$ and $B$ particles be ($az$) and ($bz$) respectively. Equations [15] to [18] then become:

$$zan_A = 2n_{AA} + n_{AB} \quad [31]$$

$$zbn_B = 2n_{BB} + n_{AB} \quad [32]$$

and

$$2Y_A = 2X_{AA} + X_{AB} \quad [33]$$

$$2Y_B = 2X_{BB} + X_{AB} \quad [34]$$

The molar enthalpy of mixing and molar excess entropy (per mole of components $A$ and $B$) become:

$$\Delta H^M = \left(b_AX_A + b_BX_B\right)\left(X_{AB}/2\right)\omega \quad [35]$$

$$\Delta S^E = -\frac{Rz}{2}\left(b_1X_1 + b_2X_2\right)\left(\begin{array}{l} X_{11}\ln\dfrac{X_{11}}{X_1^2} + X_{22}\ln \\ \dfrac{X_{22}}{X_2^2} + X_{12}\ln\dfrac{X_{12}}{2X_1X_2}\end{array}\right) \quad [36]$$

$$+\left(b_1X_1 + b_2X_2\right)\left(X_{12}/2\right)\eta$$

In the ideal entropy term, however, we do not replace $X_A$ and $X_B$ by $Y_A$ and $Y_B$, but we retain the expression:

$$\Delta S^{ideal} = -R\left(X_A\ln X_A + X_B\ln X_B\right) \quad [37]$$

in order that when ($\omega$ - $T\eta$) = 0 the equations reduce to the ideal solution equations. In order to choose the composition of maximum ordering, it is only the ratio $a/(a + b)$ which must be fixed. For example, the choice $a = 2$, $b = 4$ or the choice $a = 1$, $b = 2$ will both give $Y_A = Y_B = 1/2$ at $X_A \approx 2/3$. As before, however, we may apply the additional condition that $\Delta S = 0$ when $\omega = -\infty$ at the composition of maximum ordering ($Y_1 = Y_2 = 1/2$). This condition is satisfied when:

$$b_2 z = -\left[\ln(r) + \left(\frac{1-r}{r}\right)\ln(1-r)\right]/\ln 2 \quad [38]$$

$$b_1 = b_2 r/(1-r) \quad [39]$$

where $r = a/(a + b)$ is the ratio required to fix the composition of maximum ordering.

### Composition dependence of $\omega$ and $\eta$

The final modification to the quasi-chemical model concerns the composition dependence of $\omega$ and $\eta$. Constant values may be sufficient to represent the main features of the curves of $\Delta H^M$ and $\Delta S^E$ for ordered systems, but for a quantitative representation of the thermodynamic properties of real systems it is necessary to introduce an empirical composition dependence. Pelton and Blander[3] chose simple polynomial expansions in the equivalent fraction $Y_B$:

$$\eta = \eta_o + \eta_1 Y_B + \eta_2 Y_B^2 + \eta_3 Y_B^3 + \ldots \quad [40]$$

$$\omega = \omega_o + \omega_1 Y_B + \omega_2 Y_B^2 + \omega_3 Y_B^3 + \ldots \quad [41]$$

where the temperature- and composition-independent coefficients $\omega_1$ and $\eta_1$ are chosen empirically to give the best representation of the available experimental data for a system. When $(\omega - \eta^T)$ is small, then the excess configurational entropy is also small and $X_{AB} \approx 2X_A X_B$. (For simplicity, let $a = b = 1$ so that $X_A = Y_A$ and $X_B = Y_B$). In this case:

$$\Delta H^M \approx X_A X_B\left(\omega_o + \omega_1 X_B + \omega_2 X_B^2 + \ldots\right) \quad [42]$$

$$S^E \approx X_A X_B\left(\eta_o + \eta_1 X_B + \eta_2 X_B^2 + \ldots\right) \quad [43]$$

These equations are identical to the enthalpy of mixing and the excess entropy expressed as polynomial expansions in the mole fractions of the components.

Therefore, as the solution approaches ideality, the present model approaches the simple and common representation of excess properties by polynomial expansions and the coefficients $\omega_i$ and $\eta_i$ become numerically equal to the coefficients of these expansions.

### Partial molar properties

Expressions for the partial molar Gibbs energies of the components are obtained by differentiation:

$$\Delta\overline{G}_A = RT\ln a_A = RT\ln X_A + \frac{az}{2} \quad RT\ln\frac{X_{AA}}{Y_A^2} - a\left(\frac{X_{AB}}{2}\right)Y_B\frac{\partial(\omega - \eta T)}{\partial Y_B} \quad [44]$$

$$\Delta\overline{G}_B = RT\ln a_B = RT\ln X_B + \frac{bz}{2} \quad RT\ln\frac{X_{BB}}{Y_B^2} - b\left(\frac{X_{BB}}{2}\right)Y_A\frac{\partial(\omega - \eta T)}{\partial Y_B} \quad [45]$$

where $a_A$ and $a_B$ are the activities of the components.

### The modified quasi-chemical theory for ternary solutions

The modified quasi-chemical equations may be extended to multicomponent systems in a straightforward manner. Consider a ternary solution with mole fractions $X_A$, $X_B$, $X_C$. Equivalent fractions $Y_A$, $Y_B$, $Y_C$ may be defined as:

$$Y_A = \frac{aX_A}{aX_A + bX_B + cX_C} \quad [46]$$

$$Y_B = \frac{bX_B}{aX_A + bX_B + cX_C} \quad [47]$$

$$Y_C = \frac{cX_c}{aX_A + bX_B + cX_C} \quad [48]$$

For the various nearest-neighbour pairs $i$–$j$ we defined pair mole fractions $X_{ij}$ as before. Mass balance considerations then give, by extension of Equations [33] and [34]:

$$2Y_A = 2X_{AA} + X_{AB} + X_{CA} \quad [49]$$

$$2Y_B = 2X_{BB} + X_{AB} + X_{BC} \quad [50]$$

$$2Y_C = 2X_{CC} + X_{CA} + X_{BC} \quad [51]$$

The functions $\omega_{AB}$, $\omega_{BC}$, $\omega_{CA}$ and $\eta_{AB}$, $\eta_{BC}$, $\eta_{CA}$ are the molar enthalpy and nonconfigurational entropy changes for the three pair exchange reactions as in Equation [10].

The ternary enthalpy of mixing and excess entropy is then given by:

$$\Delta H^M = \left(aX_A + bX_B + cX_C\right)\left(X_{AB}\omega_{AB} + X_{BC}\omega_{BC} + X_{CA}\omega_{CA}\right)/2 \quad [52]$$

$$\Delta S^E = -\frac{Rz}{2}\left(aX_A + bX_B + cX_C\right)\times\left(X_{AA}\ln\frac{X_{AA}}{Y_A^2} + X_{BB}\ln\frac{X_{BB}}{Y_B^2} + X_{CC}\ln\frac{X_{CC}}{Y_C^2} + X_{AB}\ln\frac{X_{AB}}{2Y_AY_B} + X_{BC}\ln\frac{X_{BC}}{2Y_BY_C} + X_{CA}\ln\frac{X_{CA}}{2Y_CY_A}\right) + \left(aX_A + bX_B + cX_C\right)\left(X_{AB}\eta_{AB} + X_{BC}\eta_{BC} + X_{CA}\eta_{CA}\right)/2 \quad [53]$$

By minimizing the total Gibbs energy at constant composition, three equations similar to Equation [24] are generated:

$$\frac{X_{ij}^2}{X_{ii}X_{jj}} = 4e^{-2\left(\omega_{ij} - \eta_{ij}T\right)/zRT} \quad [54]$$

The functions $\omega_{ij}$ and $\eta_{ij}$ are the polynomial expansions in the three binary subsystems which can be obtained by analysis of the measured binary data. In order to be able to estimate the thermodynamic properties of the ternary from the binary data, it is necessary to approximate $\omega_{ij}$ and $\eta_{ij}$ in the ternary system from their values in the binaries.

Two methods that suggest themselves are illustrated in Figure 3. In the 'symmetric approximation', $\omega_{ij}$ and $\eta_{ij}$ are assumed to be constant along lines of constant molar ration $Y_i/Y_j$, while in the 'asymmetric approximation' $\omega_{AB}$ and $\omega_{CA}$ (and $\eta_{AB}$ and $\eta_{CA}$) are constant at constant $Y_A$, while $\omega_{CA}$ (and $\eta_{CA}$) are constant at constant $Y_B/Y_C$.

With values of $\omega_{ij}$ and $\eta_{ij}$ in the ternary obtained by one of these approximation techniques, the three Equations [54] can be solved simultaneously with Equations [49] through [51] to give the six bond fractions $Xij$ which can then be

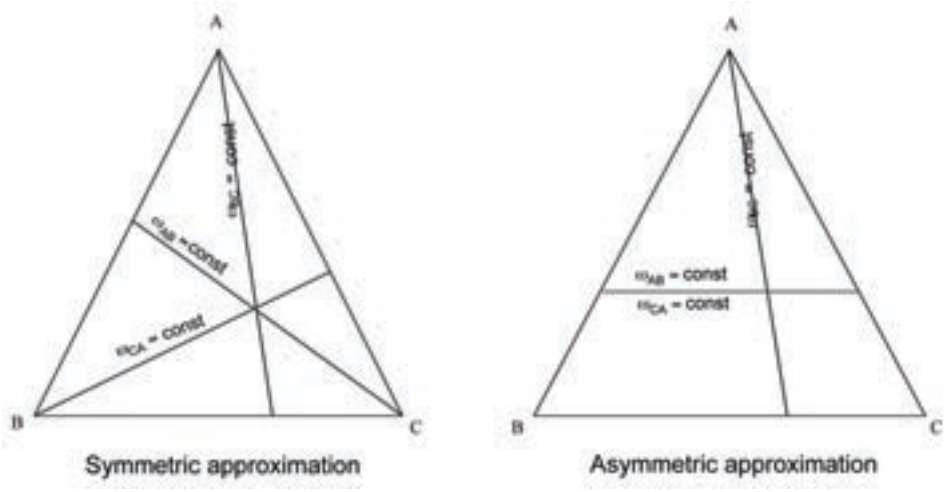


**Figure 3—Two methods to approximate $\omega_{ij}$ and $\eta_{ij}$ in the ternary system from their values in the binaries**

substituted into Equations [52] and [53] to give $\Delta H$ and $SE$. The calculation is similar to a simultaneous complex chemical equilibrium calculation and can be solved by similar computer algorithms.

The properties of ternary phases may be approximated from the assessed parameters of the binary subsystems in this manner. If experimental ternary data are available, then the approximations may be refined by the addition of 'ternary terms' to the Gibbs energy expression such as $\phi_{ijk}X^i_A X^j_B X^k_C$ where $i$, $j$, $k$ are all positive non-zero integers and where $\phi_{ijk}$ are adjustable ternary parameters. Ideally the model should be good enough so that such ternary terms should be small, or not necessary at all.

Extension of the equations of this section to systems with more than 3 components is straightforward. The solution of the resultant set of equations for the 'complex quasi-chemical equilibria' can be solved by computer algorithms.

### *Partial molar properties*

Expressions for ternary partial molar properties of the components may be obtained by differentiation. In the symmetric approximation:

$$\Delta\overline{G}_A = RT\ln a_A = RT\ln X_A + \frac{az}{2}RT\ln\frac{X_{AA}}{Y_A^2} - a\left(\frac{X_{AB}}{2}\right)\frac{Y_B}{\left(Y_A+Y_B\right)^2}\frac{\partial\left(\omega_{AB}-\eta_{AB}T\right)}{\partial\left[Y_B/\left(Y_A+Y_B\right)\right]} \quad [55]$$

and similarly for $\Delta\overline{G}_B$ and $\Delta\overline{G}_C$.

In the asymmetric approximation Equation [44] becomes:

$$\Delta\overline{G}_A = RT\ln a_A = RT\ln X_A + \frac{az}{2}RT\ln\frac{X_{AA}}{Y_A^2} + a\left(\frac{1-Y_A}{2}\right)\left[\begin{array}{l} X_{AB}\dfrac{\partial\left(\omega_{AB}-\eta_{AB}T\right)}{\partial Y_A} + X_{CA} \\ \dfrac{\partial\left(\omega_{CA}-\eta_{CA}T\right)}{\partial Y_A}\end{array}\right] \quad [56]$$

$$\Delta\overline{G}_B = RT\ln a_B = RT\ln X_B + \frac{az}{2}RT\ln\frac{X_{BB}}{Y_B^2} + b\left(\frac{1-Y_A}{2}\right)\left[\begin{array}{l} X_{AB}\dfrac{\partial\left(\omega_{AB}-\eta_{AB}T\right)}{\partial Y_A} + X_{CA} \\ \dfrac{\partial\left(\omega_{CA}-\eta_{CA}T\right)}{\partial Y_A}\end{array}\right] \quad [57]$$

$$\Delta\overline{G}_B = RT\ln X_B + \frac{bz}{2}RT\ln\frac{X_{BB}}{Y_B^2} + b\left(\frac{X_{BC}}{2}\right)\frac{Y_C}{\left(Y_B+Y_C\right)^2}\frac{\partial\left(\omega_{BC}-\eta_{BC}T\right)}{\partial\left[Y_C/\left(Y_B+Y_C\right)\right]}$$

And similarly for $\Delta\overline{G}_C$.

## The cell model

### *Background*

Yokokawa and Niwa[5] first developed a model using the concept of oxygen and cation sub-lattices. Later Kapoor and Frohberg[6] developed a similar model, but it had no applications beyond a few ternary systems. This model was then extended by Gaye and co-workers[2] to represent the properties of multi-component systems in terms of only binary parameters. Hongjie Li[7] extended this model further to accommodate not only oxygen, but any number of anionic species.

To date, the model has been primarily applied to slags in the composition range of steelmaking slag. It has been successful in predicting the distribution ratios of sulphur and phosphorus between metal and slag and it proved very reliable in multi-component systems.

### *The model structure*

This model uses a concept of oxygen and cation sub-lattices. The cation sub-lattice is filled in decreasing order of cation charge. A liquid mixture of $m$ oxides in which $X_i$ represents the mole fraction of oxide $(M_i)u_i \cdot O_{vi}$ ($i$ = 1 to $m$) is

considered. The structure is described in terms of symmetric (*i–O–i*) and asymmetric (*i–O–j*) cells. This oversimplified picture has no claim to represent the actual polymeric structure of the melt. However, on the example of the CaO-$SiO_2$ system, a (*Si–O–Si*) cell represents a double bonded ($O^0$) oxygen, a (*Si–O–Ca*) cell represents a singly bonded oxygen ($O^-$) and a (*Ca–O–Ca*) cell represents a free oxygen ion ($O^{2-}$). The computed numbers $R_{Si\text{-}Si}$ and $2_{RSi\text{-}Ca}$ of (*Si–O–Si*) and (*Si–O–Ca*) cells will reflect the degree of polymerization.

To each asymmetric cell is associated its energy of formation, $W_{ij}$ from the symmetric cells constituting the limiting pure liquid oxides.

$$i-O-i \; + \; j-O-j \; = \; 2i-O-j \left(\rightarrow 2W_{ij}\right) \quad [58]$$

It was necessary to consider a linear variation of $W_{ij}$ with composition: $W_{ij} = (W_{ij})_1 + (W_{ij})_2 \cdot X_i$ where *i* is the cation of highest charge.

The various cells are assumed to be distributed randomly and interaction energies between them are considered (e.g. $E_{ij\text{-}kl}$ to represent interaction energy between cells *i–O–j* and *k–O–l*). Further assumptions are made, which allow the consideration of only binary interaction parameters:

Interaction between like cells is neglected. 'Addition rules' are assumed, such as

$$E_{ii-ij} \; = \; 2E_{ii-ij} \quad [59]$$

$$E_{ij-kk} \; = \; E_{ik-kk} \; + \; E_{jk-kk} \; ;... \quad [60]$$

The only remaining type of interaction parameter ($E_{ij\text{-}ii}$) will be called $E_{ij}$. As with the energy of formation, a linear relationship was considered:

$$E_{ij} = \left(E_{ij}\right)_1 + \left(E_{ij}\right)_2 \cdot X_i \quad [61]$$

Thus, the model was designed with the objective to describe multi-component systems only in terms of a few binary parameters. These parameters were taken as temperature independent. No ternary interactions are taken in to account and the interaction and formation energies are functions of a simple linear model with only two parameters. This can be compared to the polynomial expansions of quasi-chemical model parameters, $\omega$ and $\eta$ in Equations [40] and [41], with parameters $\omega_0$, $\omega_1$, $\omega_2$... $\omega_n$ and $\eta_0$, $\eta_1$, $\eta_2$ ...$\eta_m$.

### *Expression of the thermodynamic functions of the liquid mixture of oxides*

The free energy of mixing is expressed by the following equation:

$$G^M = 2\sum_{i=1}^{m-1}\sum_{j=i+1}^{m}\left[R_{ij}W_{ij} + R_{ii}\frac{v_j \cdot X_j}{D_1}E_{ij}\right] - RT\sum_{i=1}^{m-1}\frac{u_i}{v_i}\left[D_i \ln\left(\frac{D_i}{v_i X_i}\right) - D_{i+1}\ln\left(\frac{D_{i+1}}{v_i X_i}\right)\right] - RT\sum_{i=1}^{m}\sum_{j=1}^{m}\left[R_{ij}^* \ln R_{ij}^* - R_{ij}\ln R_{ij}\right] \quad [62]$$

where the cell fractions, $R_{ij}$ satisfy a system of $m(m+1)/2$ constraints ($i$ = 1 to $m$).

$$\sum_{j=1}^{m} R_{ij} = v_i X_i \quad [63]$$

$$R_{ii} \cdot R_{jj} - R_{ij}^2 / P_{ij}^2 - 0 \; \left(j = i+1 \text{ to } m\right) \quad [64]$$

The linear Equations [63] are material balances and the quadratic Equations [64] come from the maximization of the partition function.

The enthalpy and entropy of mixing are obtained using the Gibbs-Helmholtz equation.

$$H^M = \partial\left(G^M/T\right) / \partial\left(1/T\right) \quad [65]$$

$$S^M = \left(H^M - G^M\right)/T \quad [66]$$

When $E_{ij}$ and $W_{ij}$ are assumed temperature independent, the mixing entropy is identical to the configurational entropy. The component activities are calculated with the following equation.

$$RT\ln a_i = G^M + \sum_{j=2}^{m}\left(\delta_{ij} - X_j\right)\partial G^M / \partial X_j \; (i = 1 \text{ to } m) \quad [67]$$

where $\delta_{ij}$ represents Kronecker's delta symbol which takes on a value of 1 when $j = i$ and zero elsewhere.

The derivatives of the free energy of mixing, can be calculated numerically:

$$\partial G^M / \partial X_j = \left[\begin{matrix} G^M\left(X_k, X_j + \Delta X_j\right) - G^M \\ \left(X_k, X_j - \Delta X_j\right)\end{matrix}\right] / 2\Delta X_j \quad [68]$$

Changes of the reference state can then be made to express the activities with respect to the classically used reference state, e.g.

$$\left(a_{MO_s}\right) / \left(a_{MO_l}\right) = \exp\left(\frac{\Delta H_m - T\Delta S_m}{RT}\right) \quad [69]$$

$\Delta H_m$ and $\Delta S_m$ in this equation are the enthalpy and entropy of melting of the pure component.

The slag model has been successfully applied to steel-making slags and has been used by IRSID[8] as a standard modelling method.

To estimate $E_{ij}$ and $W_{ij}$ (also $\omega$ and $\eta$ for the quasi-chemical model), data from literature is required. It is very important that a positive number of degrees of freedom are maintained by having more datasets than model parameters.

### Data from the literature

All available data in literature have to be critically reviewed before any of it can be used as researchers may publish conflicting results. Due to the extreme experimental difficulties in working and containing Fe-Ti-O slags at high temperature, the number of experimental data points are limited (in comparison to Ca-Mg-Al-Si-O slag systems).

### *The FeO–$TiO_2$ binary system*

The first attempt to measure liquidus points in the FeO–$TiO_2$

binary system was made by Grieve and White[9]. Thermal studies were carried out by the differential thermocouple method, using tungsten-molybdenum thermocouples. Their diagram showed two intermediate components (pseudo-brookite and ilmenite), both melting at approximately 1470°C. They indicated high uncertainty in the high $TiO_2$ region.

MacChesney and Muan[10] determined phase relations in the Fe–Ti–O system by the quenching technique. Mixtures of iron oxide and titanium oxide were equilibrated under carefully controlled atmospheres and then quenched rapidly to room temperature. The phases present were identified by microscopic and X-ray examination. From their results, they added a third congruently melting component, pseudo-brookite, to their diagram. They stated that Grieve and White[9] misnamed $2FeO.TiO_2$ as pseudobrookite and they named it ulvospinel. MacChesney and Muan[10] added some ranges of solubility to their intermediate components as well as to rutile and wüstite.

In 1979 Grau[11] performed some cooling curve experiments. In the technique Grau[11] used, the slag temperature is continuously recorded during a cooling cycle and the liquidus temperature is determined from the arrest in the time-temperature curve, which indicates the beginning of crystallization. He showed that pseudobrookite melts incongruently, forming rutile and liquid slag via a peritectic reaction. The high titanium side of the $FeO–TiO_2$ phase diagram was amended by Berman and Brown[12] who calculated the heat capacity equations for several minerals including ilmenite and pseudobrookite using the low temperature data of Shomate[13] and the high temperature data from Naylor[14].

### *The Ti–$TiO_2$ system*

De Vries and Roy[15] first established the phase diagram for the Ti–$TiO_2$ system. They observed that rutile was reduced in air and darkened on heating above 1500°C. They also found that the oxygen:titanium ratio of the rutile phase varied between 1.99:1 and 1.95:1. They concluded that rutile was a solid solution phase between $TiO_2$ and $Ti_3O_5$ with a eutectic reaction at 1830°C.

Wahlbech and Gilles[16] reinvestigated the Ti–$TiO_2$ system, incorporating more recent data. They also measured chemical equilibrium data in the titanium monoxide region. Wahlbech and Gilles[16] accepted a much smaller homogeneity range for $Ti_2O_3$ and an even smaller one for $Ti_3O_5$. Wahlbeck and Gilles[16] also included the Magnéli phases between $Ti_3O_5$ and $TiO_2$. The so-called Magnéli phases are represented by the general formula $Ti_nO_{2n-1}$ with the value of $n$ ranging from 4 to 10. A more resent assessment of the system was done by Murray and Wriedt[17].

Waldner and Eriksson[18] used all available T-x phase diagram and thermodynamic data (about 600 points) to calculate the Gibbs free energies of 18 phases. Twelve of these phases were treated as line components. The complete Ti-O system was assessed, including gaseous oxygen and Magnéli phases, between 298 K and the liquidus temperature and at a pressure of 1 bar. The model parameters for all the different phases were computed by an optimization procedure for finding the best fit to the experimental information. These calculations were carried out with the Gibbs energy minimization program ChemSage and produced the optimized phase diagram (Figure 4).

### Data used in this optimization

No single source contains all the relevant data to the required degree of accuracy; consequently the number of different sources used in this optimization. The same models and thermodynamic data were used for the solid phases throughout this modelling, while the MQC and cell solution models were each evaluated for the liquid slag. The thermodynamic properties of $TiO_2$, $Ti_2O_3$ and FeO (values of $\Delta H°_{298}$, $S°_{298}$ and Cp (s)) were taken from Eriksson and Pelton[19]. They did a critical assessment of all available thermodynamic and phase diagram data and used only the most accurate and reliable data in their optimizations.

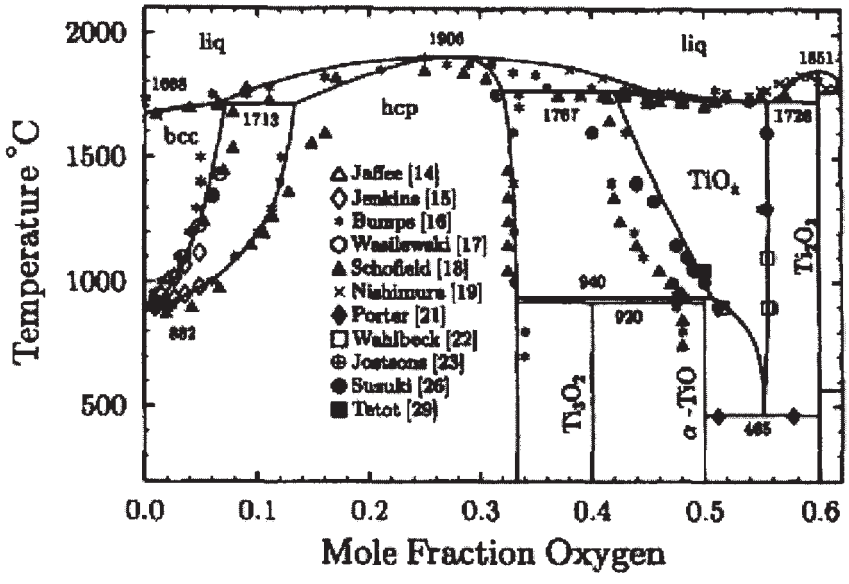


**Figure 4—The Ti-$TiO_2$ phase diagram proposed by Waldner and Erikson[18]**

### $TiO_2$

The melting point of $TiO_2$ was taken to be 1870°C from Brauer and Littke[20]. An expression for Cp(l) was derived from data in the JANAF Thermochemical Tables[21] by Eriksson and Pelton[19] and used in this optimization. Below 2130 K, Cp(l) was set to be equal to Cp(s).

### $Ti_2O_3$

The melting temperature was taken from the JANAF Thermochemical Tables[21] as 2115 ± 10 K. The values of $\Delta H°_{298}$, $S°_{298}$, $\Delta H°_m$, $S°_m$ were also taken from the JANAF Thermochemical Tables[21]. Expressions for Cp were fitted to the data in these tables by Eriksson and Pelton[19]. Below 2115 K, Cp(l) was set equal to Cp(s).

### FeO

The thermodynamic properties of 1 mol solid FeO were obtained from Eriksson and Pelton[19] who added the values of the molar enthalpy, entropy and heat capacity of $Fe_{0.947}O$ to those of 0.053 mol of Fe. The melting point of 1644 K was adopted from the data of MacChesney and Muan[10]. Below 1644 K, Cp(l) was set equal to Cp(s).

### $TiO_2$–$Ti_2O_3$

The oxides from $Ti_2O_3$ to the 'last' of the Magnéli phases, '$Ti_{20}O_{39}$', were described as line components, as was done by Waldner and Eriksson[18]. Magnéli phases are defined as $Ti_nO_{2n-1}$, where $n \geq 4$ and ranges to values above $n = 20$. These phases have a crystal structure derived from the rutile phase by crystallographic shear. The maximum value of $n$ is not yet determined and therefore an arbitrary value of $n = 20$ was chosen to represent all the phases where $n > 10$. The most complete and consistent liquidus measurements are those of Brauer and Littke[20]. These data points were obtained by optical techniques and were used in this optimization.

### $TiO_2$–FeO

The data used in this optimization were the low titanium data from MacChesney and Muan[10], that is, the melting point of FeO, 1644 K and the melting point of Ulvospinel, 1670 K. On the high titanium side, ten data points from Grau[11] were used. Two points on the pseudobrookite/liquid phase boundary and eight points on the rutile/liquid boundary. All the Cp equations from the JANAF Thermochemical Tables[21] were also used.

### $Ti_2O_3$–FeO

In this binary system there is believed to exist a reaction-equilibrium rather than a phase-equilibrium. This equilibrium can be described by the following reaction:

$$Fe^{2+} + Ti^{3+} \rightleftarrows Fe^0 + Ti^{4+} \qquad [70]$$

From this equation it is clear that FeO and $Ti_2O_3$ cannot co-exist without the formation of $TiO_2$ and therefore the $Ti_2O_3$–FeO binary exists only as part of the $TiO_2$–$Ti_2O_3$–FeO ternary.

### $TiO_2$–$Ti_2O_3$–FeO

According to Nell[22], no unique ternary compounds exist in this system.

## Results

### The FeO–$TiO_2$ binary

The model parameters were calculated using a parameter optimisation routine built into the ChemSAGE package and the results are shown in Figure 5.

Eriksson and Pelton[19] have done the optimization of the same system using their modified quasi-chemical model. They got a similar fit to the data (Figure 6) with also some deviation at the high titanium end. Only two quasi-chemical parameters for the liquid were required in this optimization (note the nonlinear polynomial dependence):

$$\omega = -12405 - 10227 Y^2_{TiO_2} \cdot \qquad [71]$$

Both models showed some deviation at higher $TiO_2$ values. This could be as a result of $Ti_2O_3$ formation during the experiments. If this were the case, the experimental error would increase and both the models would be well within the error limit. The RMS (root mean square) error for the cell model and the MQC model was 23.9°C and 18.8°C, respectively.

### The $TiO_2$–$Ti_2O_3$ binary

Pelton and Eriksson[19] again did the optimization of the system for the MQC model. They indicated an unsure region in the low $TiO_2$ part of the diagram (Figure 7). The form of the curve in this region indicates a higher order expansion of the model parameters and could be interpreted as curve-fitting. The following quasi-chemical parameters were obtained from the optimization:

$$\omega = 18913 - 175126\ Y_{TiO_2} + 338410\ Y^2_{TiO_2} - 177916\ Y^3_{TiO_2} \cdot \qquad [72]$$

The cell model (Figure 8) predicted a much wider region of $Ti_3O_5$ + liquid than the MQC model and a smaller two-phase region for the $Ti_2O_3$ + liquid region. The eutectic's position has shifted to 30% $TiO_2$ (compared to 42% for the MQC model). The predicted eutectic temperature shifted down from about 1680°C to 1660°C. The RMS (root mean square) error for the Cell model and the MQC model was 32°C and 17°C, respectively, for this binary system.

### The $TiO_2$–$Ti_2O_3$-FeO ternary

The only ternary data found in the literature was measured by Pesl and Eric[23]. They postulated the following liquidus isotherms at 1500°C and 1600°C for the $TiO_2$-$TiO_{1.5}$-FeO ternary (Figure 9). They measured the liquid slag phase boundary by means of saturation experiments. The oxygen isobars within the slag phase are also indicated on the diagram.

The data points measured by Pesl and Eric[23] were plotted on a new set of coordinates, to be able to compare it to the diagrams produced by the software packages. It is more common to use $Ti_2O_3$ rather than $TiO_{1.5}$ used by Pesl and Eric[23].

The liquidus isotherm at 1500°C for the $TiO_2$-$Ti_2O_3$-FeO system was calculated using the MQC model and was compared to the data points measured by Pesl and Eric[23] (Figure 10). It can be seen that the basic form is retained,

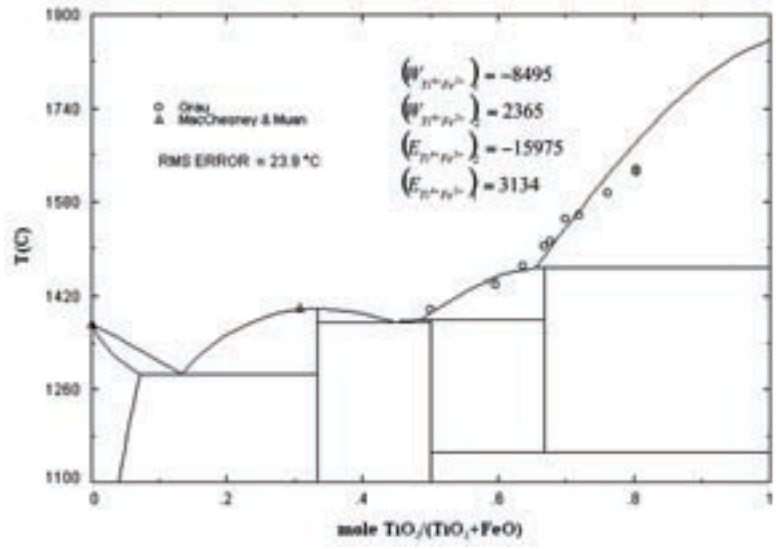


**Figure 5—$FeO-TiO_2$ phase diagram as calculated by the cell model**

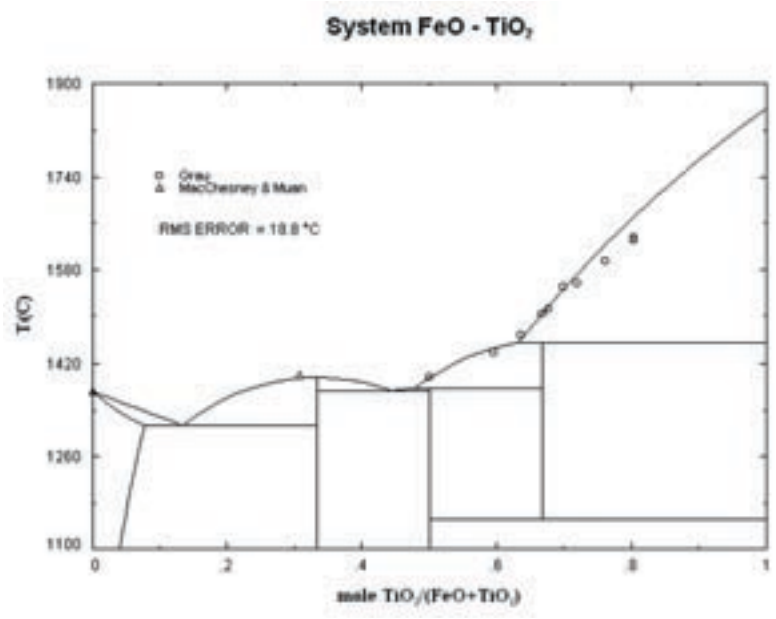


**Figure 6—$FeO-TiO_2$ phase diagram as calculated by the modified quasi-chemical model**

although the liquid slag region is much smaller. In this case all the Magnéli phases, as well as the pseudobrookite phase was taken as line components and no solubility range was allowed for.

The remaining four interaction parameters could now be regressed by keeping the eight binary interaction parameters already optimized constant and using all the binary and ternary data points available. The interaction parameters obtained from this optimization were then used to draw the 1500°C isotherm for the $TiO_2$–$Ti_2O_3$–FeO ternary system. The liquidus isotherm calculated using the MQC model (Figure 10) could now be compared directly with the same isotherm calculated using the cell model and the newly regressed model parameters (Figure 11).

The two ternary phase diagrams compare well, mostly due to the fact that the same solid solution models and pure component data were used and that all the Magnéli phases were assumed to be line components.

The optimized binary interaction parameters were then used to generate a liquidus projection of the $TiO_2$-$Ti_2O_3$-FeO system (Figure 12).

This plot was then repeated (Figure 13) using the MQC model for the slag phase.

From the direct comparison between the liquidus projections using the cell model and the MQC models (Figures 12 and 13, respectively), it can be seen that the MQC model predicts a slightly bigger slag liquid region at higher temperatures. A visual comparison shows that both models compare poorly at 1500°C for two experimental data points in the range 0.11–0.17 mole fraction $Ti_2O_3$, where the model predicts the liquidus isotherm in the region of a $Ti_2O_3$ molefraction of 0.05. In both cases, the slag stability region is

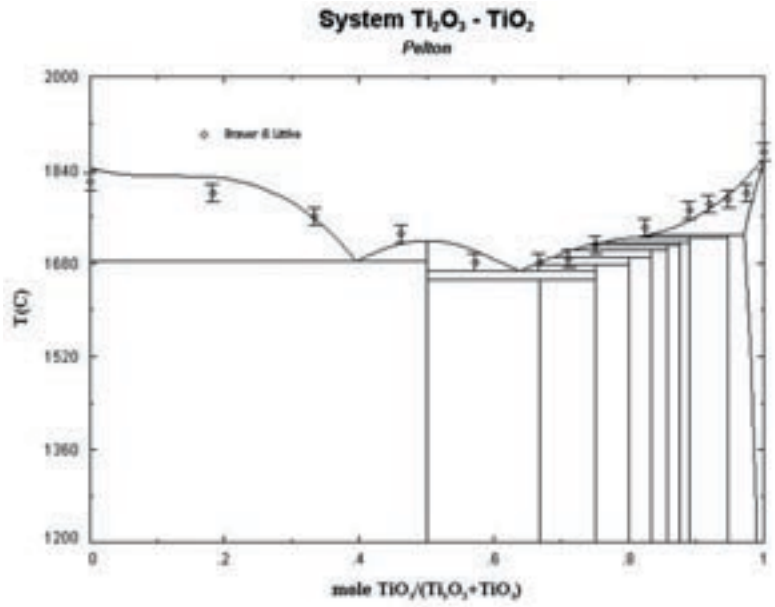


**Figure 7—$TiO_2$-$Ti_2O_3$ phase diagram as calculated by the modified quasi chemical model**

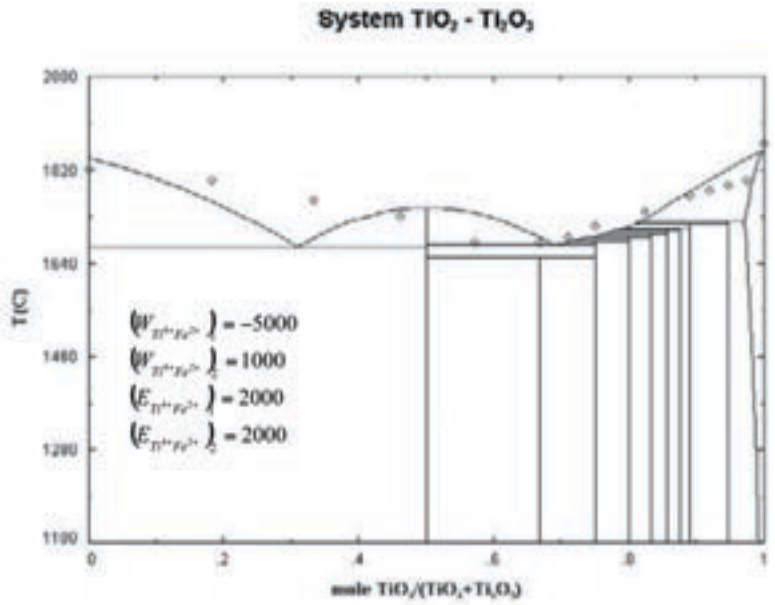


**Figure 8—$TiO_2$-$Ti_2O_3$ phase diagram as calculated by the cell model**

smaller than those noted experimentally. On the other hand, the cell model performs quite well when the data points at 1600°C are compared to the model-predicted 1600°C isotherm. The MQC model significantly overestimated the region where the slag phase is predominant and does not compare as well with the measured data.

Table I gives a comparison of the interaction parameters as determined for the cell model.

A comparison of the relative magnitudes of the interaction parameters presented in Table I shows that the $FeO$-$Ti_2O_3$ pseudo-binary shows the strongest interaction and can be related to their tendency to react, as well as to their attraction to form $Fe^{2+}$-$Ti^{3+}$ minerals, temperature permitting. The $TiO_2$-$Ti_2O_3$ system shows the weakest interaction, as can be expected when compared to the dissimilar Fe-Ti systems. It is clear that all the interaction parameters are linear in terms of composition, with a minimum number of parameters, and is consequently simpler than the MQC model structure, while maintaining a similar level of model accuracy.

## Conclusions

In this article, two well-known slag models were described and used to model the ternary $TiO_2$-$Ti_2O_3$-$FeO$ system. The modified quasi-chemical Model (MQC) has been developed over the past few years and has been optimized for this particular system, while the cell model has previously been

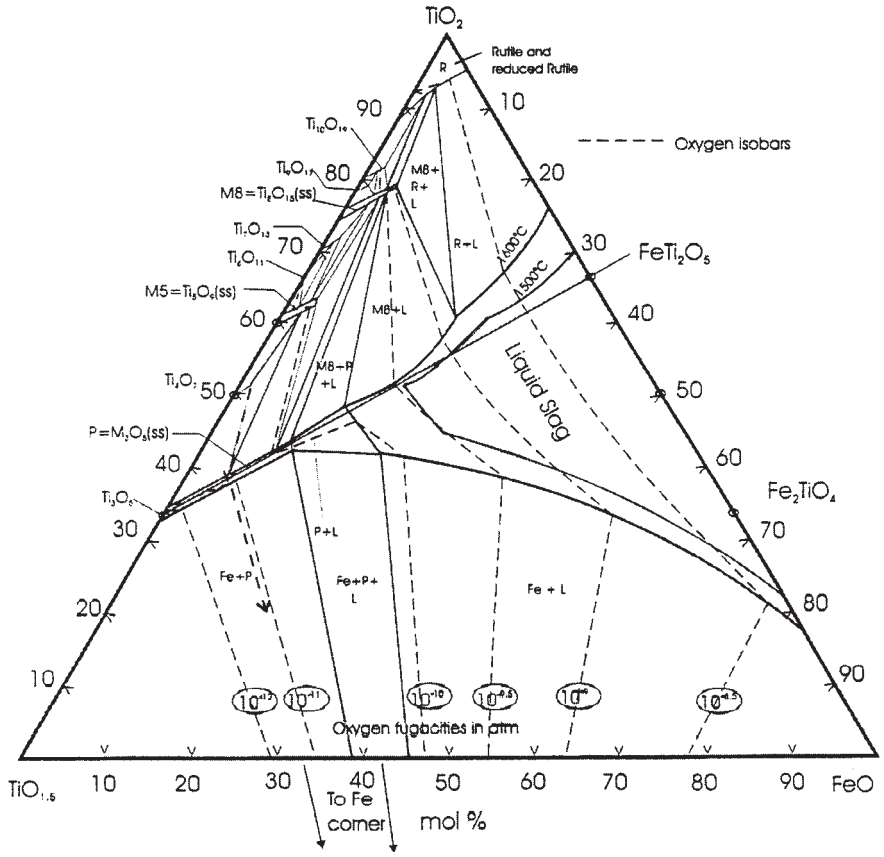


**Figure 9—The liquidus isotherm at 1500°C and 1600°C for the $TiO_2$-$TiO_{1.5}$ FeO ternary after Pesl and Eric[23]**

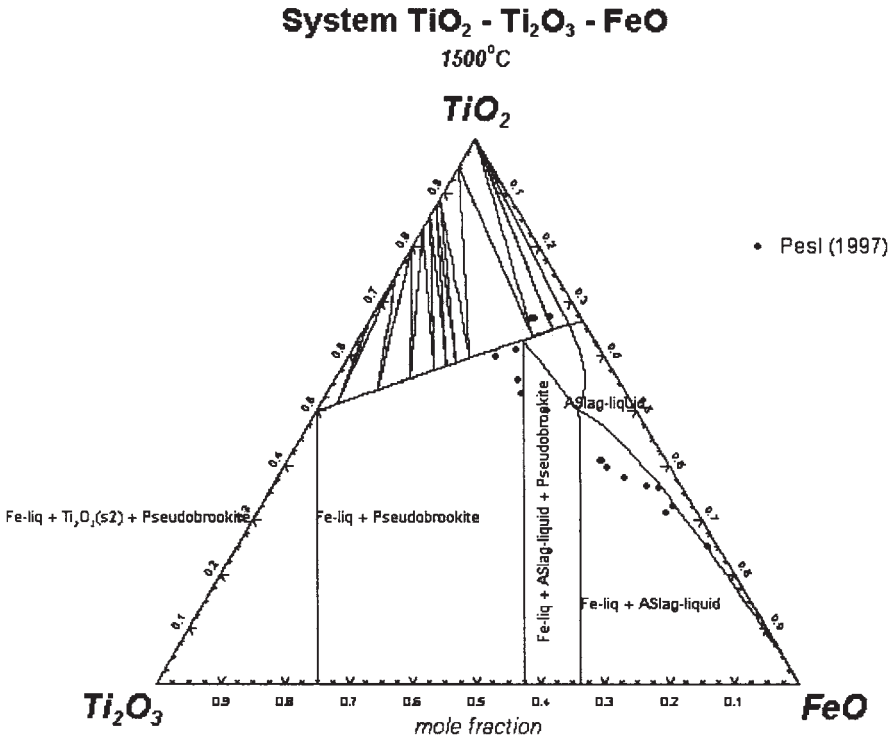


**Figure 10—An isothermal section at 1500°C for the $TiO_2$-$Ti_2O_3$-FeO ternary as calculated using the MQC model combined with the measured data points by Pesl[24]**

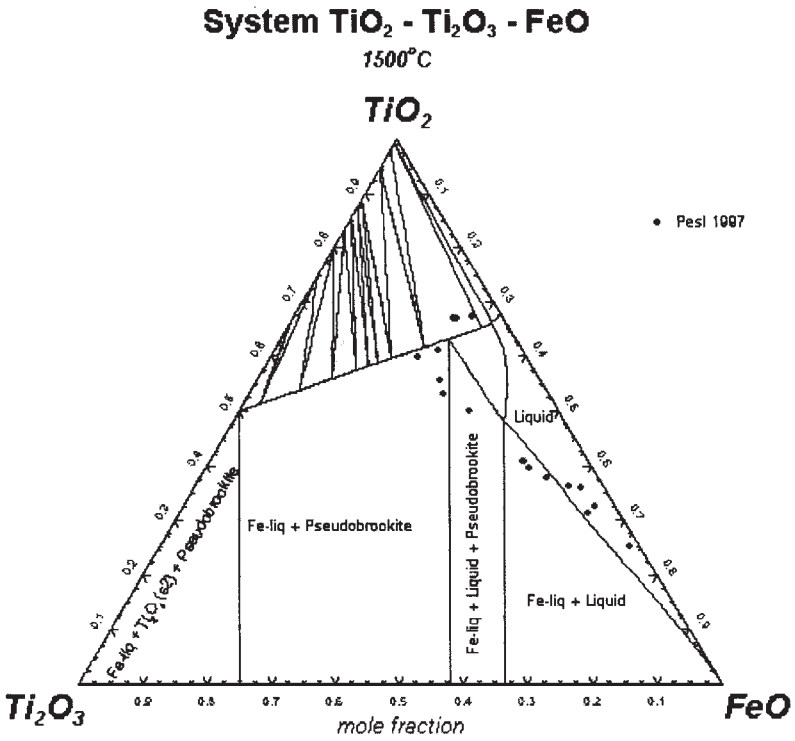


**Figure 11—An isothermal section at 1500°C for the $TiO_2$-$Ti_2O_3$-FeO ternary system as calculated using the cell model combined with the measured data points by Pesl[24]**

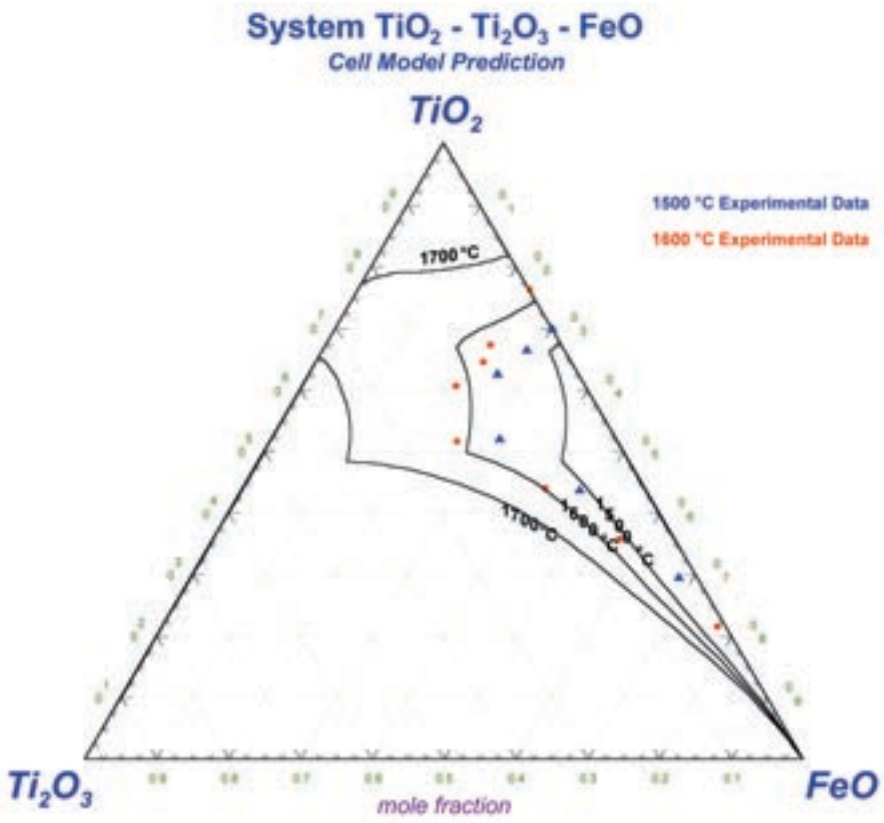


**Figure 12—Liquidus isotherms of the $TiO_2$-$Ti_2O_3$-FeO ternary system using the cell model to describe the liquid slag phase**

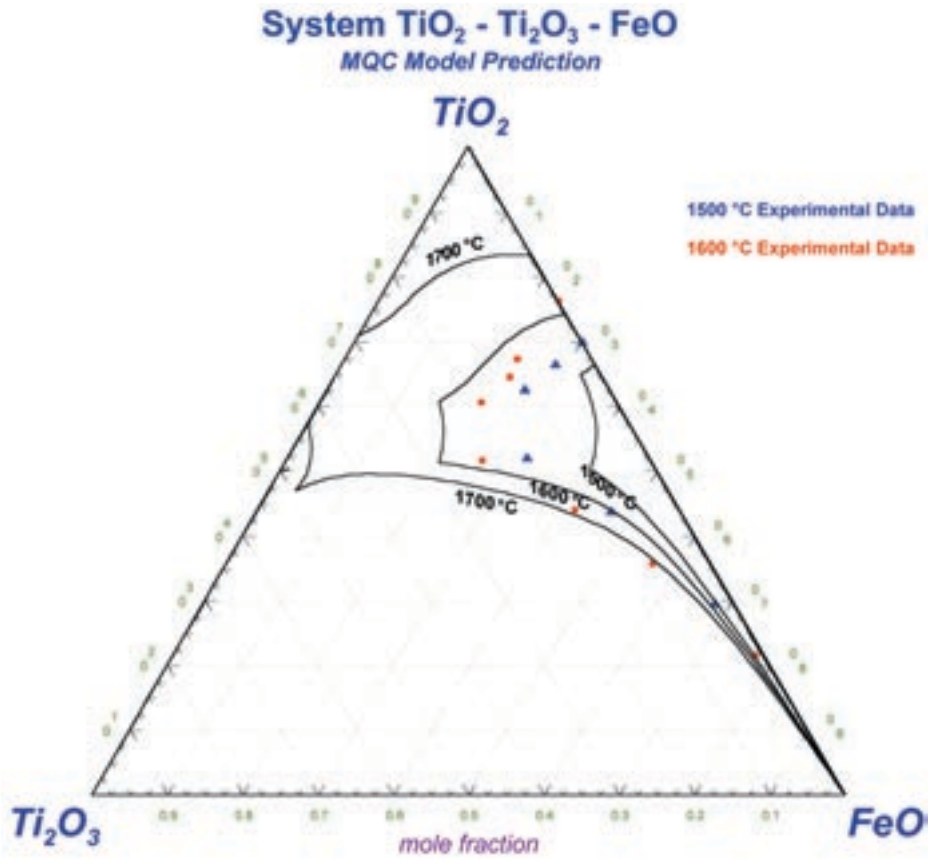


**Figure 13—Liquidus isotherms of the $TiO_2$-$Ti_2O_3$-FeO system using the modified quasi-chemical model to describe the liquid slag phase**

*Table I*

**Summary of the cell model binary interaction parameters**

| | | FeO–$TiO_2$ | $TiO_2$-$Ti_2O_3$ | FeO-$Ti_2O_3$ |
|---|---|---|---|---|
| Cell Model | $E_{ij}$<br>$W_{ij}$ | 3100 – 16000 $X_{Ti4+}$<br>-8500 + 2400 $X_{Ti4+}$ | 2000 + 2000 $X_{Ti4+}$<br>-5000 + 1000 $X_{Ti4+}$ | -10000 + 10000 $X_{Ti3+}$<br>- 20000 |

used only in steelmaking slags. The optimizations done in this study, shows that the cell model could be used with great success for the modelling of ionic melts like the high titanium slag investigated in this work. It further highlights the importance of accurate and reliable thermodynamic data, for the use in optimizing model parameters. Although both models have a fundamental and statistical thermodynamics' backbone, it still relies heavily on good data to be able to calculate the interaction parameters. These solution models, together with their derived interaction parameters and mineral pure component data, can be subsequently implemented in software, which makes use of Gibbs energy minimization to predict phase and reaction equilibria. The cell model is typically implemented in the CSIRO MPE® (multiphase equilibrium) software[25], while the MQC model has been implemented in FactSage® by CRCT[26]. The information presented in this paper can therefore contribute to the slag solution databases of the above-mentioned software.

## Significance and application

The use of accurate solution models to describe the thermodynamic behaviour of melts is indispensable in the process modelling of metallurgical plants as these models are required to:

- predict the activities of the components in the melt, which, in turn, are used to determine the distribution ratio of components in the slag to components in the alloy according to chemical reaction equilibrium between the alloy and slag
- predict the phase equilibria of melts and, moreover, determine the type of minerals that precipitate, the chemistry of the remaining melt (fully liquid component) and the fraction of the bulk slag that has crystallized. The fraction of the bulk melt that has crystallized is important because the type of solid (and therefore its density) will determine if the solids will float (forming a crust on the slag), will sink (forming a

'false bottom' in the furnace) or, when the crystal density is similar to the liquid slag portion, will remain suspended in the slag melt. In this last-mentioned case, it contributes significantly to the viscosity of the melt. The influence of the fraction of precipitated minerals to the liquid-only portion on the observed bulk viscosity can be estimated with the Einstein-Roscoe equation[27]. The equation estimates the ratio of the bulk (solid + liquid) viscosity to the liquid-only portion, which takes on the general form:

$$\mu_R = \frac{\mu_S}{\mu_L} = \left(1 - R \cdot \Phi_S\right)^{-n} \qquad [73]$$

where $R$ and $n$ are empirical parameters which equal 1.35 and 2.5, respectively, for spheres of equal size and 1 and 2.5 respectively, for rigid spheres of diverse sizes, and was found to provide a good fit to experimental data on viscosity of 2-phase crystallized melts[27]. However, needle-like crystals are expected to deviate significantly, and Equation [73] is expected to give the lower estimate of viscosity, as this class of crystals (to which minerals precipitating from the high titania slags belong) tend to interlock at a much looser packing than the corresponding packing that can be achieved with spherical or isometric minerals. Lastly, viscosity itself is one of the most critical melt properties to control to ensure slag tappability, control over slag foaming, and metal entrainment en massetransfer in the slag.

Accurate prediction of the slag liquidus allows one therefore to link it to the slag chemistry and, via the material and energy balances, to the feed and power input to a furnace. It is also critical for good slag freeze lining control.

## Acknowledgements

The authors would like to thank Mintek for their financial support.

## Nomenclature

$i,j$ - components
$m$ - number of components
$i$–$j$ - nearest-neighbour pairs
$a_i$ - activity of component $i$
$\sigma_{ij}$ - pair bond non-configurational entropy
$n_i$ - number of moles of $i$
$n_{ij}$ - number of moles of $i$–$j$ pairs
$v_i$, $u_i$ - stoichiometric indexes
$R_{ii}$, $2R_{ij}$ - numbers of $i$–$O$–$i$, $i$–$O$–$j$ cells
$R^*_{ij} = (v_i v_j X_i X_j)/D_1$ - fraction of $i$–$O$–$j$ cells for a random distribution of cations on their sublattice

$$D_i = \sum_{k=i+1}^{m} v_k X_k$$

$$Q_i = \sum_{k=i+1}^{m} (v_k X_k / D_1)\,(E_{ik} / RT)$$

$$P_{ij} = \begin{cases} 1 & \text{if } (j = i) \\ \exp(Q_i).\exp(Q_j)\exp(-W_{ij}/RT) & \text{if } (j \neq i) \end{cases}$$

$\Omega_i$ - $\Omega_i = n_i!/(n_{ii}!(n_i - n_{ii})!)$
$\varepsilon_{ij}$ - pair bond energies
$\phi_{ijk}$ - adjustable ternary parameters

$$\delta_{ij} = \begin{cases} 1 & (i = j) \\ 0 & (i \neq j) \end{cases}$$ Kronecker's delta function

$\eta$ - molar non-configurational entropy change (MQC model)
$\mu_R$ - ratio of bulk viscosity to liquid-only viscosity
$\mu_S$ - bulk slag viscosity (including solids)
$\mu_L$ - slag viscosity of liquid-only portion
$\Phi$ - volume fraction of solids in bulk slag
$\omega$ - molar enthalpy change (MQC model)
$z$ - lattice co-ordination number
$a,b$ - integers
$r = a/(a + b)$
$E_{ij} = (E_{ij})_1 + (E_{ij})_2 \cdot X_i$ - energy parameters for cells' interaction (cell model)
$W_{ij} = (W_{ij})_1 + (W_{ij})_2 \cdot X_i$ - energy parameters for asymmetric cells, formation (cell model)
$k$ - Boltzmann's constant
$N^0$ - Avogadro's number
$n$ - parameter of viscosity equation
$R$ - parameter of viscosity equation
$T$ - absolute temperature
$T_{mA}$ - melting temperature of $A$
$X_i$ - mole fractions
$X_{ij}$ - mole fractions of each type of pair in solution
$Y_i$ - equivalent fractions
$\Delta$ - delta (change in, or difference)
$C_P$ - heat capacity at constant pressure
$H$ - enthalpy
$S^E$ - excess entropy
$H°_{fus}$ - enthalpy of fusion
$S°_{fus}$ - entropy of fusion
$H_m$ - enthalpy of melting of the pure component
$S_m$ - entropy of melting of the pure component
$H°_{298}$ - enthalpy of formation at 298 K
$S°_{298}$ - entropy of formation at 298 K
$G_i$ - Gibbs free energy of component $i$

## References


1. GUOCHANG, J, KUANGOLI, X. and SHOUKUN, W. Some advances on the theoretical research of slag, *ISIJ International*, vol. 33, 1993, pp. 20–25.

2. GAYE, H. and WELFINGER, J. Modelling of the Thermodynamic Properties of Complex Metallurgical Slags, *Second International Symposium on Metallurgical Slags and Fluxes*, H.A. Fine and D.R. Gaskell (eds.) Warrendale, PA. The Metallurgical Society of AIME, 1984, pp. 357–375.

3. PELTON, A.D. and BLANDER, M. Thermodynamic Analysis of Ordered Liquid Solutions by a Modified Quasichemical Approach—Application to Silicate Slags, *Metallurgical and Materials Transactions B*, vol. 17B, 1986, pp. 805–815.

4. GUGGENHEIM, E.A. The Statistical Mechanics of Regular Solutions, *Proc. Roy. Soc.*, vol. A148, 1935, pp. 304–312.

5. YOKOKAWA, T. and NIWA, K. *Transactions of the Japanese Institute of Metals*, vol. 10, 1969, pp. 3, 81.

6. KAPOOR, M.L. and FROHBERG, M.G. Theoretical treatment of activities in Silicate melts, *Chemical metallurgy of iron and steel*, The Iron and Steel Institute, London, 1973, pp. 17–22.

7. LI, H. Computer Assisted Thermodynamic Studies on Metallurgical Processes Focused on Recycling, PhD thesis, University of Tohoku, Japan, 1995.

8. GAYE, H., RIBOUD, P.V., and WELFINGER, J. Use of a slag model to describe slag-metal reactions and precipitations of inclusions, *Ironmaking and Steelmaking*, vol. 15, 1988, pp. 319–322.

9. GRIEVE, J. and WHITE, J. The System $FeO-TiO_2$, *Journal of the Royal Technical College*, vol. 4, 1939, pp. 441–448.

10. MACCHESNEY, J.B. and MUAN, A. Phase Equilibria at Liquidus temperatures in the System Iron Oxide-Titanium Oxide at Low Oxygen Pressures, *American Mineralogist*, vol. 46, 1961, pp. 572–582.

11. GRAU, A.E. Liquidus Temperatures in the $TiO_2$-rich side of the $FeO-TiO_2$ System, *Canadian Metallurgical Quarterly*, vol. 18, 1979, pp. 313–321.

12. BERMAN, R.G. and BROWN, T.H. Heat capacity of minerals in the system $Na_2O-K_2O-CaO-MgO-FeO-Fe_2O_3-Al_2O_3-SiO_2-TiO_2-H_2O-CO_2$: representation, estimation and high temperature extrapolation, *Contributions to Mineral Petrology*, vol. 89, 1985, pp. 168–183.

13. SHOMATE, C.H. Heat capacities at low temperatures of titanium dioxide (rutile and anatase), *American Chemical Society Journal*, vol. 69, 1947, pp. 218–219.

14. NAYLOR, B.F. High-temperature heat contents of TiO, $Ti_2O_3$, $Ti_3O_{.5}$ and $TiO_2$, *American Chemical Society Journal*, vol. 68, 1946, pp. 1077–1080.

15. DE VRIES, R.C. and ROY, R. A Phase Diagram for the System $Ti–TiO_2$ Constructed from Data in the Literature, *American Ceramic Bulletin*, 1954, pp. 370–372.

16. WAHLBECK, P.G. and GILLES, P.W. Reinvestigation of the Phase Diagram for the System Titanium–Oxygen, *Journal of The American Ceramic Society*, vol. 49, 1966, pp. 180–183.

17. MURRAY, J.L. and WRIEDT, H.A. The O-Ti (Oxygen-Titanium) System, *Bulletin of Alloy Phase Diagrams*, vol. 8, 1987, pp. 148–165.

18. WALDNER, P. and ERIKSSON, G. Thermodynamic Modelling of the System Titanium-Oxygen, *CALPHAD*, vol. 23, 1999, pp. 189–218.

19. ERIKSSON, G. and PELTON, A.D. Critical Evaluation and Optimisation of the Thermodynamic Properties and Phase Diagrams of the $MnO-TiO_2$, $MgO-TiO_2$, $FeO-TiO_2$, $Ti_2O_3-TiO_2$, *and* $K_2O-TiO_2$ Systems, *Metallurgical and Materials Transactions B*, vol. 24B, 1993, pp. 795–805.

20. BRAUER, G. and LITTKE, W. Über den Schmelzpunkt und die Thermische Dissoziation von Titandioxyd, *J. Inorg. Nucl. Chem.*,vol. 16, 1960, pp. 67–76

21. JANAF Thermochemical Tables, 3rd ed., *J. Phys. Chem. Ref. Data*, vol. 14, 1985.

22. NELL, J. *The Journal of the South African Institute of Mining and Metallurgy*, Johannesburg, vol. 100, 2000. pp. 35–44.

23. PESL, J. and ERIC, R.H. High Temperature Phase Relations and Thermodynamics in the Iron-Titanium-Oxygen System, *Metallurgical and Materials Transactions B*, vol. 30B, pp. 695–705, 1999.

24. PESL, J. Thermodynamics and phase equilibria in the FeO–Ti–O system at 1500°C and 1600°C and metal-slag-equilibria pertinent to ilmenite smelting, PhD thesis, University of the Witwatersrand, South Africa, 1997.

25. ZHANG, L., JAHANSHAHI, S., SUN, S., CHEN, C., BOURKE, B., WRIGHT, S., and SOMERVILLE, M. CSIRO's Multiphase Reaction Models and Their Application, *Journal of Metals*, vol. 54 no. 11, 2002, pp. 51–56.

26. BALE, C.W., CHARTRAND, P., DEGTEROV, S.A., ERIKSSON, G., HACK, K., BEN MAHFOUD, R., MELANÇON, J., PELTON, A.D., and PETERSEN, S, FactSage Thermochemical Software and Databases, *Calphad*, vol. 26, no.2, 2002, pp. 189–228.

27. ROSCOE, R. *British Journal of Applied Physics*, vol. 3, 1952, pp. 267–269. u